

Electrochemical Investigation on the Stable Iron Species in Molten FLINAK

Hao Peng^{1,2}, Miao Shen¹,
Chenyang Wang¹, Yong Zuo¹
and Leidong Xie¹

Abstract

The electrochemical behavior of Fe(III) in molten LiF–NaF–KF [46.5:11.5:42 (mol%)] [FLINAK] salt was studied by cyclic voltammetry (CV), chronopotentiometry (CP) and square wave voltammetry (SWV) at 600°C. It was found that Fe(III) was initially reduced to Fe(II) at +2.0 V (vs. alkalis) followed by reduction of Fe(II) to Fe at +1.4 V (vs. alkalis) and both reduction processes were controlled by ion diffusion. Diffusion coefficients of Fe(III) in molten FLINAK were calculated through CV and CP. The reduction peak of Fe(III)/Fe(II) was still observed in SWVs even though only FeF₂ was added to FLINAK. This result showed that Fe(II) was converted to Fe(III), which exists stably in FLINAK melts.

Keywords: Molten fluorides; Stable iron valence; Cyclic voltammetry; Chronopotentiometry; Square wave voltammetry

- 1 Shanghai Institute of Applied Physics, Chinese Academy of Sciences, Shanghai, PR China
- 2 University of Chinese Academy of Sciences, Beijing, PR China

Corresponding author: Leidong Xie

✉ xieleidongsinap@163.com

Shanghai Institute of Applied Physics,
Chinese Academy of Sciences, Shanghai
201800, PR China.

Tel: +8602139194105

Fax: +8602139194105

Citation: Peng H, Shen M, Wang C, et al. Electrochemical Investigation on the Stable Iron Species in Molten FLINAK. *Insights Anal Electrochem.* 2016, 2:1

Received: January 11, 2016; **Accepted:** January 25, 2016; **Published:** January 31, 2016

Introduction

Molten fluorides are suitable for use as coolants of molten salt reactors because these materials present excellent heat transfer properties [1-3]. However, the residual oxidation of impurities in fluorides, such as absorbed water and HF(g) [4,5], are corrosive to the structural materials at high temperature [6-9], resulting in the dissolution of Fe in those materials [10], such as Hastelloy.

According to the investigations described by Oak Ridge National Laboratory (ORNL) [11], the corrosion valence state of Fe in molten fluorides is determined by the acid-base properties of the molten fluoride employed; here, a Lewis acid is defined as a fluoride ion acceptor, and a Lewis base is a fluoride ion donor. Pure FLINAK consisting of LiF, NaF, and KF [LiF:NaF:KF, 46.5:11.5:42 (mol%)] is known to be a strongly basic solvent that tends to stabilize the Fe(III) valence state [11]. According to the theory of non-electric transfer described by Ozeryanaya [12], Fe may firstly dissolve in FLINAK melts as a form of Fe(II), which would further convert to Fe(III). Unfortunately, no relevant studies have yet been published to prove this conversion.

By using cyclic voltammetry (CV), Bing [13] found that Fe(III) could be converted to Fe(II) in KCl–CaCl₂–NaCl–MgCl₂ melts. With the same method, Manning [14] indicated that O₂²⁻ and O₂²⁻ ions stayed stable in LiF–BeF₂–ZrF₄ and LiF–BeF₂–ThF₄ melts whereas O₂⁻ was unstable in these eutectics. Recently, Nourry [15] found that U(III) could be oxidized to U(IV) in LiF–CaF₂–UF₃ melts through CV and SWV. Cassayre and Pakhui [16,17] claimed that

Th(IV) is the only stable species in LiCl–KCl melts at 420–550 °C by involving CV, CP, SWV and chronoamperometry (CA). Reports thus far [13-19] suggest that the electrochemical method can be used to investigate the stable valence of electro-active species because the technique offers quick responses and *in-situ* monitoring. The aim of the present work is to determine the stable valence state of Fe in FLINAK melts through CV, CP and SWV.

Experimental Methods

Highly-purified LiF–NaF–KF [46.5:11.5:42 (mol%)] [FLINAK] eutectic salt was used as the experimental fluorides. A known amount of Fe(III) and Fe(II) were introduced to FLINAK salt as the form of FeF₃ (Strem Chemicals, 99.9%) and FeF₂ (Alfa Aesar, 99%), respectively. Then the fluorides system was melted at 600°C in a vitreous carbon crucible placed in a stainless steel cell inside an electric furnace. The temperature of the melts was measured by a nickel-chromium thermocouple positioned just outside the crucible.

A platinum wire ($\Phi=1.0$ mm) served as the working electrode, whose surface area was determined by measuring the immersion depth in the melts. A graphite rod ($\Phi=6.0$ mm) was used as

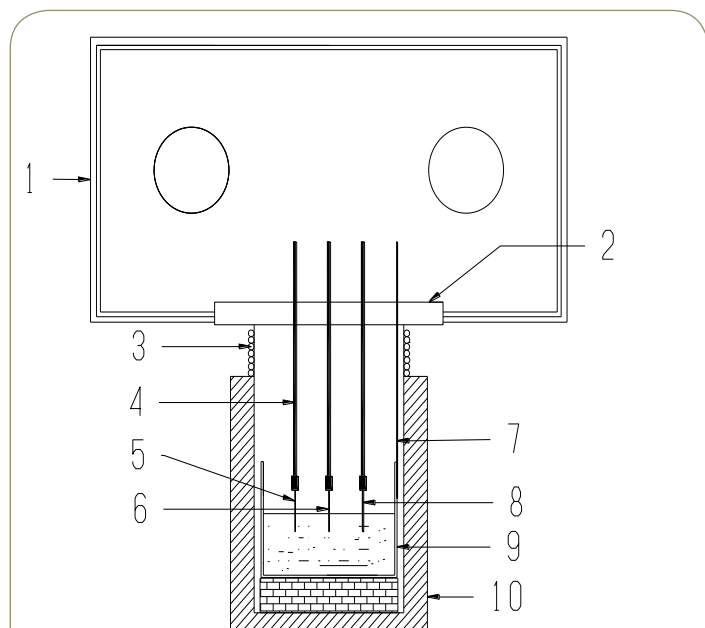
the auxiliary electrode with a large surface area (2.50 cm²). All potentials were referred to a platinum wire ($\Phi=1.0$ mm) that had been proven to function as a quasi-reference electrode Pt/PtOx/O²⁻, with a stable potential when the O²⁻ concentration is constant [20,21]. The entire apparatus was placed inside a glove box with dry argon atmosphere (99.99 wt%), as shown in **Figure 1**, and the typical concentrations of moisture and oxygen in glove box were generally below 2 ppm. All electrochemical measurements were performed with a computer-controlled AUTOLAB digital electrochemical analyzer (Metrohm AutoLab Co. Ltd.).

Results and Discussion

Electrochemical behavior of Fe(III) in FLINAK melts

Cyclic voltammetry: The typical cyclic voltammograms of FLINAK-Fe(III) (484 ppm) melts on a Pt electrode at 600°C and different scan rates are shown in **Figure 2**. Two reduction peaks, A and B, at 1.97 V (vs. alkalis) and 1.42 V (vs. alkalis), respectively, in the cathodic run and two anodic counter-peaks, A' and B', at 2.15 V (vs. alkalis) and 1.52 V (vs. alkalis), respectively, can be observed. As the Fe(III) concentration increases, the current densities of peak A and B (i_{p_A} and i_{p_B}) increase accordingly, as shown in **Figure 3**. Thus, the reduction of Fe(III) proceeds in two steps.

A/A' redox system: The cathodic current density of peak A (i_{p_A}) obtained after subtracting the background current [22,23] linearly increases with the square root of the scan rate ($v^{1/2}$) as shown in **Figure 4a**, indicating that the first reduction step of Fe(III) is controlled by ion diffusion. In addition to the almost invariable peak potential (E_{p_A}) in the range of 0.1 to 1.0 V/s, the ratio of $|i_{p_A}/i_{p_A}|$ is approximately equal to 1, as shown in **Table 1**. These



1: Glove box; 2: Transition cover; 3: Cooling coil; 4: Alumina tube; 5: Working electrode; 6: Reference electrode; 7: Thermocouple; 8: Auxiliary electrode; 9: Crucible and molten salt; 10: Furnace.

Figure 1 Schematic illustration of the electrochemical cell.

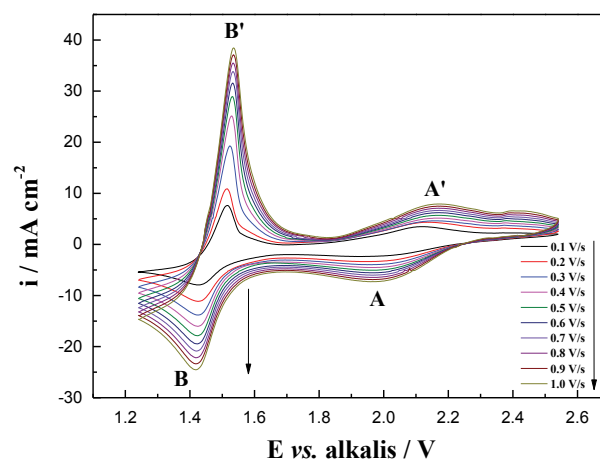


Figure 2 Cyclic voltammograms of the FLINAK-Fe(III) (484 ppm) melts at 600°C and different scan rates. Working electrode: Pt (0.62 cm²); auxiliary electrode: Graphite; reference electrode: Pt.

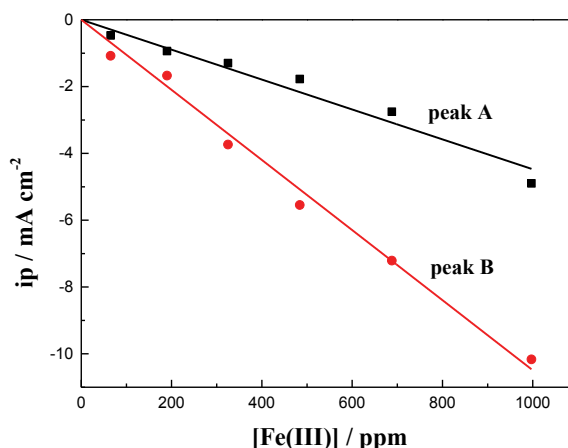


Figure 3 Linear relationship between the peak current density and Fe(III) concentration in FLINAK melts at 600°C and scan rate of 0.1 V/s for cathodic peaks A and B. Working electrode: Pt (0.62 cm²); auxiliary electrode: Graphite; reference electrode: Pt.

results suggest that the first step of Fe(III) reduction is considered reversible over the studied scan rates.

For a reversible system, the diffusion coefficient of Fe(III) in the melts can be calculated according to the Randles-Sevcik equation [24]:

$$i_p = -0.4463nFSC \left(\frac{nF}{RT} \right)^{(1/2)} D^{(1/2)} v^{(1/2)} \quad (1)$$

Where i_p is the peak current (A), n the number of exchanged electrons, F the Faraday constant (96,485 C mol⁻¹), S the electrode surface area (cm²), C the Fe(III) concentration (mol cm⁻³), R the universal gas constant (8.314 J mol⁻¹ K⁻¹), T the absolute temperature of the melts (K), D the diffusion coefficient

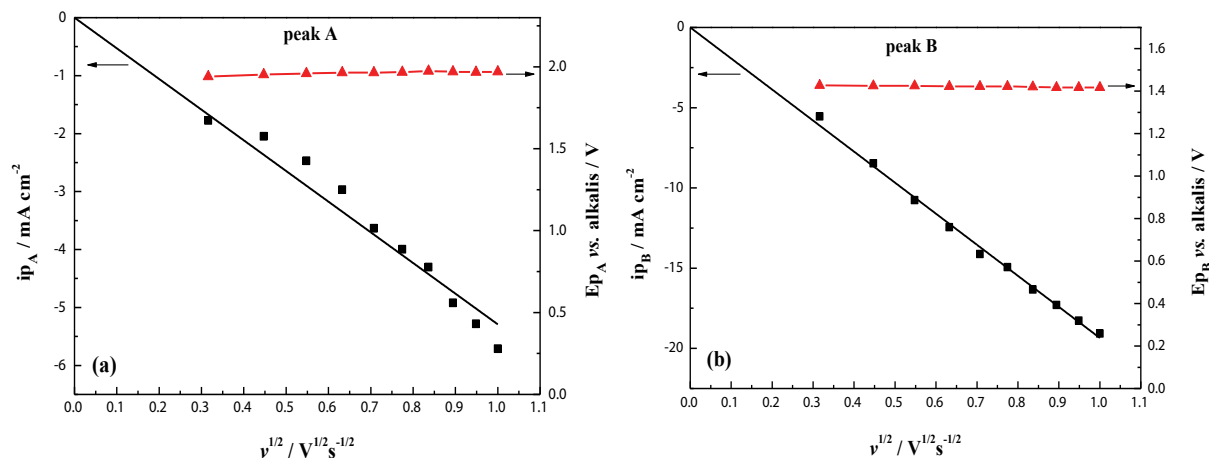


Figure 4 Plots of peak current density (ip) and peak potential (Ep) vs. the square root of the scan rate ($v^{1/2}$) for cathodic peaks A and B in FLINAK-Fe(III) (484 ppm) melts at 600°C. Working electrode: Pt (0.62 cm²); auxiliary electrode: Graphite; reference electrode: Pt.

Table 1 Ratios of the anodic to the cathodic peak current density $|ip_A/ip_B|$.

$v/V s^{-1}$	0.1	0.2	0.3	0.4	0.5	0.6	0.7	0.8	0.9	1.0
$ ip_A/ip_B $	1.28	1.06	1.17	1.10	0.93	0.99	1.06	1.02	1.04	0.99

(cm² s⁻¹) and v the potential scan rate (V s⁻¹).

The slope of ip versus $v^{1/2}$ attributed to peak A obtained in **Figure 4a** is:

$$\frac{ip}{v^{1/2}} = -0.00529 A s^{1/2} v^{-1/2} cm^{-2} \quad (2)$$

at $T=600^\circ C$ and $C=1.73 \times 10^{-5} mol cm^{-3}$.

B/B' redox system: The sharp oxidation peak B' and the ratios of $|ip_B/ip_B'| > 1$ imply the couple B/B' may be attributed to the deposition and dissolution of Fe [25,26]. Since the peak potential Ep_B remains at about 1.42 V (vs. alkalis) and the cathodic peak current density ip_B linearly increases with $v^{1/2}$ as shown in **Figure 4b**, the reduction peak B is a quasi-reversible reaction controlled by ion diffusion.

Chronopotentiometry

A typical chronopotentiogram of FLINAK-Fe(III) (997 ppm) melts obtained for an applied current of -3.5 mA on a Pt electrode at 600°C is shown in **Figure 5**. Two plateaus, A and B, at about 1.9 V (vs. alkalis) and 1.5 V (vs. alkalis), respectively, can be observed, which confirms the two-step reduction mechanism of Fe(III) previously evidenced by CV.

The validity of the Sand's law [Eq. (3)] is verified in **Figure 6**, since the $i\tau^{1/2}$ plotted versus the applied current (i) is constant [Eq. (4), (5)]. The two reduction processes of Fe(III) are thus controlled by ion diffusion in molten FLINAK. The diffusion coefficient of Fe(III) can be determined using the Sand's law [24]:

$$\frac{i\tau^{1/2}}{C} = \frac{nFSD^{1/2}\pi^{1/2}}{2} \quad (3)$$

Where i is the applied current (A), τ the transition time (s), C the Fe(III) concentration (here, $C=3.56 \times 10^{-5} mol cm^{-3}$), n the number of exchanged electrons, F the Faraday constant (96,485 C mol⁻¹),

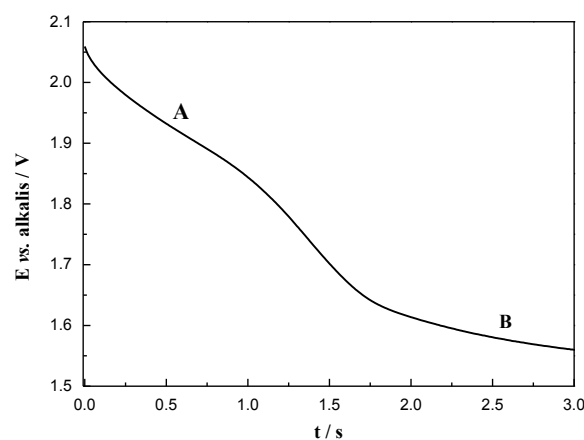


Figure 5 Chronopotentiogram of the FLINAK-Fe(III) (997 ppm) melts at 600°C when the applied current is -3.5 mA. Working electrode: Pt (0.62 cm²); auxiliary electrode: Graphite; reference electrode: Pt.

S the electrode surface area (cm²) and D the diffusion coefficient (cm² s⁻¹).

$$\text{Peak A: } i\tau^{1/2} = -0.00395 A s^{1/2} \quad (4)$$

$$\text{Peak B: } i\tau^{1/2} = -0.01242 A s^{1/2} \quad (5)$$

Number of exchanged electrons

The Fe(III) reduction mechanism was finally evidenced by calculating the number of exchanged electrons. Combining CV and CP measurements, the exchanged electron number of peak A was

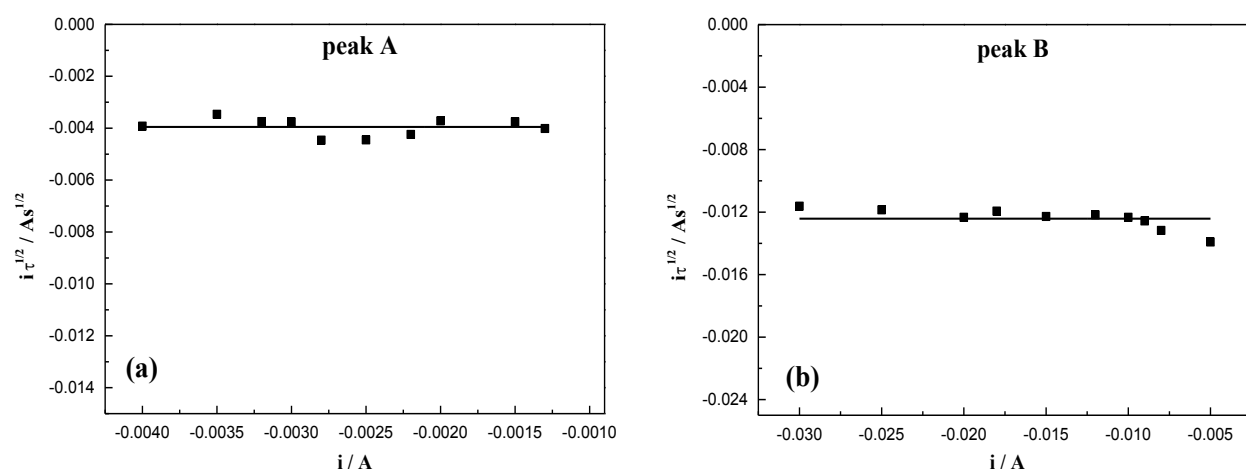


Figure 6 Dependence of $it^{1/2}$ on the applied current intensity for cathodic peaks A and B in FLINAK-Fe(III) (997 ppm) melts at 600°C. Working electrode: Pt (0.62 cm²); auxiliary electrode: Graphite; reference electrode: Pt.

obtained to be 0.87 by coupling Eq. (1)-(4). Thus, Fe(III) reduction proceeded in two steps: initial Fe(III) reduction to Fe(II) followed by subsequent reduction of Fe(II) to Fe. For the reversible Fe(III)/Fe(II) couple, Fe(III) diffusion coefficient is determined to be $3.80 \times 10^{-6} \text{ cm}^2 \text{ s}^{-1}$ from CV measurement [Eq. (1)] and to be $4.38 \times 10^{-6} \text{ cm}^2 \text{ s}^{-1}$ from CP measurement [Eq. (3)].

Square wave voltammetry

The typical square wave voltammograms of FLINAK-Fe(III) (190 ppm) melts at 30-70 Hz on a Pt electrode are shown in **Figure 7**. Two reduction peaks, A and B, at about 2.03 V (vs. alkalis) and 1.43 V (vs. alkalis), respectively, can be observed. The mathematical analysis of the peak yields a simple equation associating the width of the half peak ($W_{1/2}$) and the electron transfer number [27,28].

$$W_{1/2} = 3.52 \times \frac{RT}{nF} \quad (6)$$

Eq. (6) is theoretical valid for a reversible system, which can be extended to other systems as far as the criterion of linearity between the peak intensity and the square root of the frequency signal is respected [29-33]. As shown in **Figure 8**, the reduction peak current densities (δip_A and δip_B) show a linear relationship with the square root of the frequency. Calculated according to Eq. (6), the electron transfer number for peaks A and B are 1.04 and 1.77, respectively, as shown in **Table 2**. Thus, peaks A and B are corresponding to the reductions of Fe(III)/Fe(II) and Fe(II)/Fe, respectively. These results are in accordance with those obtained through CV and CP.

Electrochemical behavior of Fe(II) in FLINAK melts

After 740 ppm of Fe(II) was introduced into FLINAK melts in the form of FeF₂, the square wave voltammograms obtained on a Pt electrode at 600°C and different holding times are shown in

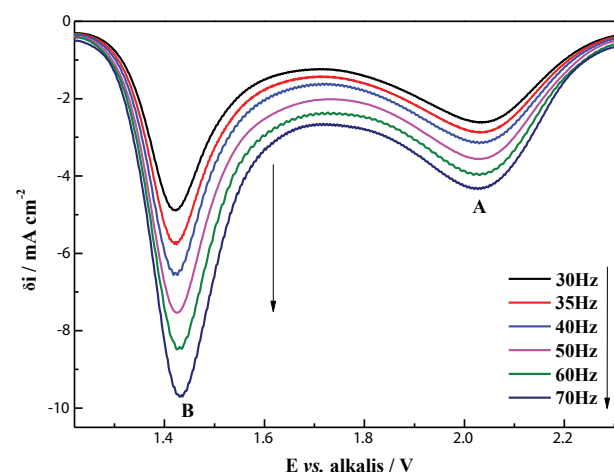


Figure 7 Square wave voltammograms of the FLINAK-Fe(III) (190 ppm) melts at 30-70 Hz and 600°C. Pulse height: 20 mV, step potential: 2 mV. Working electrode: Pt (0.62 cm²); auxiliary electrode: Graphite; reference electrode: Pt.

Figure 9. Two reduction peaks, A and B, at about 2.1 V and 1.5 V (vs. alkalis), attributed to the reductions of Fe(III)/Fe(II) and Fe(II)/Fe, respectively, can be observed. Peak A assigned to the reduction of Fe(III)/Fe(II) also appeared even though only FeF₂ was added to FLINAK, indicating the conversion of Fe(II) to Fe(III).

Plot of current density of peak A (δip_A) vs. different holding times at 600°C in FLINAK-Fe(II) (740 ppm) melts is shown in **Figure 10**. δip_A increases from -1.22 mA cm^{-2} to -5.64 mA cm^{-2} and then reaches a plateau after 130 min. The increase of δip_A before 130 min is attributed to the conversion of Fe(II) to Fe(III). After the conversion equilibrium is achieved at 130 min, the Fe(III) concentration in molten FLINAK remains constant, resulting in an unchangeable δip_A value.

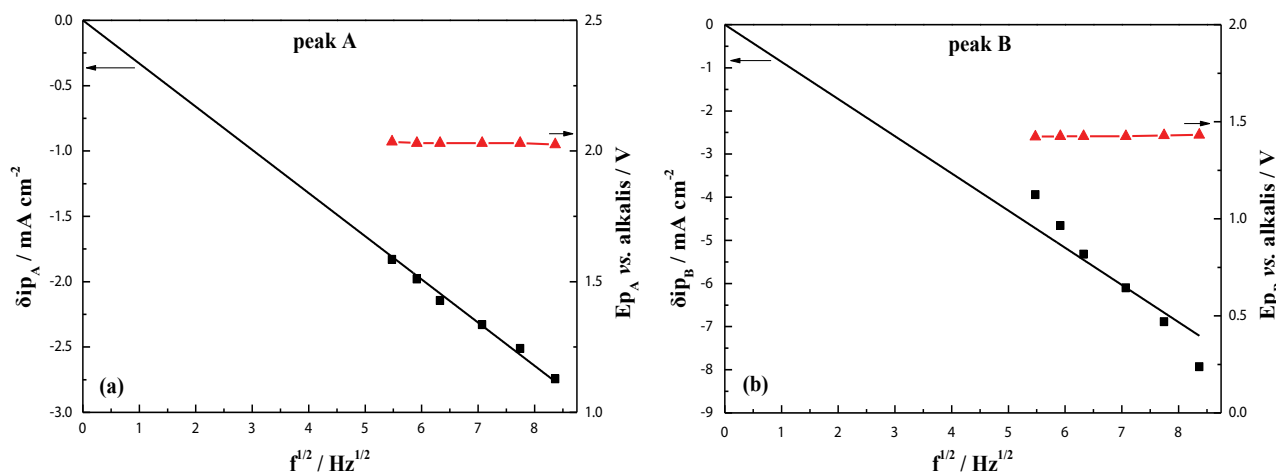


Figure 8 Plots of peak current density (δip) and peak potential (E_p) vs. the square root of the frequency ($f^{1/2}$) for cathodic peaks A and B in FLINAK-Fe(III) (190 ppm) melts at 600°C. Pulse height: 20 mV, step potential: 2 mV. Working electrode: Pt (0.62 cm²); auxiliary electrode: Graphite; reference electrode: Pt.

Table 2 Reduction reactions and electron transfer numbers of peak A and B.

Reduction peak	A	B
Reduction potential vs. alkalis	2.03 V	1.43 V
Value of $W_{1/2}$	253 mV	150 mV
Exchanged electron numbers	1.04	1.77
Corresponding reaction	Fe(III)+e=Fe(II)	Fe(II)+2e=Fe

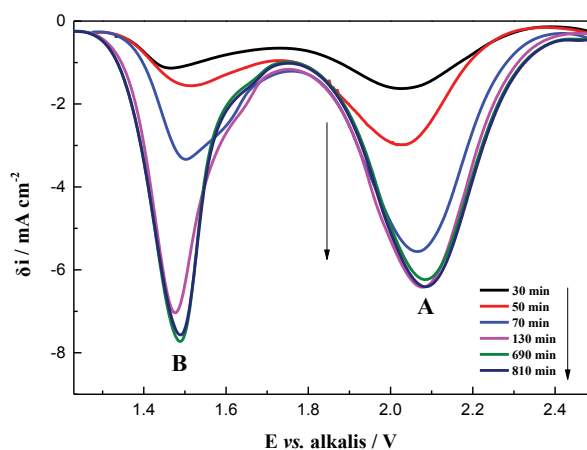


Figure 9 Square wave voltammograms of the FLINAK-Fe(II) (740 ppm) melts recorded on a Pt electrode at 600°C and different holding times. Pulse height: 20 mV, step potential: 2 mV, frequency: 10 Hz. Working electrode: Pt (0.62 cm²); auxiliary electrode: Graphite; reference electrode: Pt.

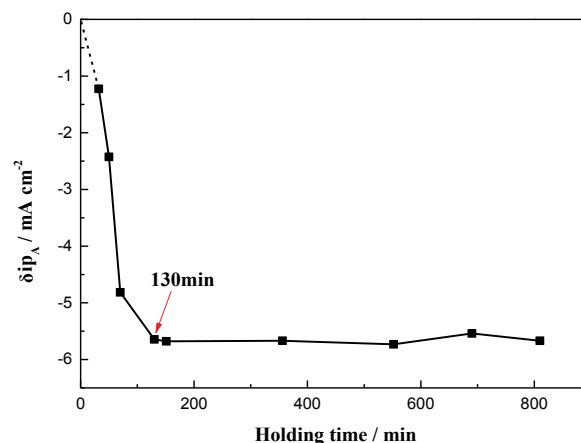


Figure 10 Plot of the current density of peak A vs. holding time at 600°C as measured from the SWVs of FLINAK-Fe(II) (740 ppm) melts. Pulse height: 20 mV, step potential: 2 mV, frequency: 10 Hz. Working electrode: Pt (0.62 cm²); auxiliary electrode: Graphite; reference electrode: Pt.

Conclusion

In this work, the electrochemical behavior of Fe(III) in molten FLINAK was studied by CV, CP and SWV. The results showed that Fe(III) was initially reduced to Fe(II), which was subsequently

reduced to Fe. Both Fe(III)/Fe(II) and Fe(II)/Fe reductions were controlled by ion diffusion. The diffusion coefficient of Fe(III) was $3.80 \times 10^{-6} \text{ cm}^2 \text{ s}^{-1}$ obtained by Randles-Sevcik equation and was $4.38 \times 10^{-6} \text{ cm}^2 \text{ s}^{-1}$ obtained by Sand's law. The electrochemical behavior of Fe(II) was then investigated by SWV. Two cathodic peaks attributed to the reductions of Fe(III)/Fe(II) and Fe(II)/Fe, can be observed. This result indicated that Fe(II) was converted to Fe(III), which is more stable in FLINAK melts.

Acknowledgements

This work was financially supported by the Strategic Priority Research Program of the Chinese Academy of Sciences (Grant No. XDA02020400) and the Young Scientists Fund of the National Natural Science Foundation of China (Grant No. 51404237).

References

- Salanne M, Simon C, Turq P, Madden PA (2009) Heat-transport properties of molten fluorides: Determination from first-principles. *J Fluorine Chem* 130: 38-44.
- Van der Meer JPM, Konings RJM (2007) Thermal and physical properties of molten fluorides for nuclear applications. *J Nucl Mater* 360: 16-24.
- Krepel J, Hombourger B, Fiorina C, Mikityuk K, Rohde U, et al. (2014) Fuel cycle advantages and dynamics features of liquid fueled MSR. *Ann Nucl Energy* 64: 380-397.
- Field PE, Shaffer JH (1967) The solubilities of hydrogen fluoride and deuterium fluoride in molten fluorides. *J Phys Chem* 71: 3218-3222.
- Shaffer JH, Grimes WR, Watson GM (1959) Solubility of hydrogen fluoride in molten fluorides. *J Phys Chem* 63: 1999-2002.
- Delpesch S, Cabet C, Slim C, Picard GS (2010) Molten fluorides for nuclear applications. *Materials Today* 13: 34-41.
- Nagasaka T, Kondo M, Muroga T, Noda N, Sagara A, et al. (2009) Fluoridation and oxidation characteristics of JLF-1 and NIFS-HEAT-2 low-activation structural materials. *J Nucl Mater* 386: 716-719.
- Kondo M, Nagasaka T, Sagara A, Noda N, Muroga T, et al. (2009) Metallurgical study on corrosion of austenitic steels in molten salt LiF-BeF₂ (Flibe). *J Nucl Mater* 386: 685-688.
- Kondo M, Nagasaka T, Xu Q, Muroga T, Sagara A, et al. (2009) Corrosion characteristics of reduced activation ferritic steel, JLF-1 (8.92Cr-2W) in molten salts Flibe and Flinak. *Fusion Eng Des* 84: 1081-1085.
- Olson LC, Ambrosek JW, Sridharan K, Anderson MH, Allen TR (2009) Materials corrosion in molten LiF-NaF-KF salt. *J Fluorine Chem* 130: 67-73.
- Williams D, Toth L, Clarno K (2006) Assessment of Candidate Molten Salt Coolants for the Advanced High-Temperature Reactor (AHTR). ORNL/TM-2006/12, Oak Ridge National Laboratory.
- Ozeryanaya IN (1985) Corrosion of metals by molten salts in heat-treatment processes. *Met Sci Heat Treat* 27: 184-188.
- Li B, Lou J, Wang H, Yu J (2011) Electrochemical investigation on stable iron ion valence in molten KCl-CaCl₂-NaCl-MgCl₂ melts. *J Rare Earth* 29: 96-98.
- Manning DL, Mamatov G (1977) Electrochemical studies of oxide ions and related species in molten fluorides. *J Electrochem Soc* 124: 480-483.
- Nourry C, Soucek P, Massot L, Malmbeck R, Chamelot P, et al. (2012) Electrochemistry of uranium in molten LiF-CaF₂. *J Nucl Mater* 430: 58-63.
- Cassayre L, Serp J, Soucek P, Malmbeck R, Rebizant J, et al. (2007) Electrochemistry of thorium in LiCl-KCl eutectic melts. *Electrochim Acta* 52: 7432-7437.
- Pakhui G, Chandra M, Ghosh S, Reddy BP, Nagarajan K (2015) Electrochemical studies on the reduction behavior of Th⁴⁺ in molten LiCl-KCl eutectic. *Electrochim Acta* 155: 372-382.
- Smirnov MV, Kudyakov VYA (1983) Thorium valency in molten alkali halides in equilibrium with metallic thorium. *Electrochim Acta* 28: 1339-1348.
- Dock CH (1965) Oxidation states of thorium in fused LiCl-KCl eutectic. Retrospective Theses and Dissertations. Paper 3910.
- Berghoute Y, Salmi A, Lantelme F (1994) Internal reference systems for fused electrolytes. *J Electroanal Chem* 365: 171-177.
- Graves AD, Inman D (1965) Adsorption and the differential capacitance of the electrical double-layer at platinum/halide metal interfaces. *Nature* 20: 481-482.
- Wang J (2000) Analytical electrochemistry. Wiley-VCH, New York, USA.
- Yoko T, Bailey RA (1984) Electrochemical studies of chromium in molten LiF-NaF-KF (FLINAK). *J Electrochem Soc* 131: 2590-2595.
- Bard AJ, Faulkner RL (1980) *Electrochemistry: Principles, Methods and Applications*. Wiley, New York, USA.
- Straka M, Korenko M, Lisy F (2010) Electrochemistry of uranium in LiF-BeF₂ melt. *J Radioanal Nucl Chem* 284: 245-252.
- Gibilaro M, Massot L, Chamelot P, Cassayre L, Taxil P (2013) Investigation of Zr(IV) in LiF-CaF₂: Stability with oxide ions and electroreduction pathway on inert and reactive electrodes. *Electrochim Acta* 95: 185-191.
- Ramaley L, Krause MS (1969) Theory of square wave voltammetry. *Anal Chem* 41: 1362-1365.
- Ramaley L, Krause MS (1969) Analytical application of square wave voltammetry. *Anal Chem* 41: 1365-1369.
- Chamelot P, Massot L, Cassayre L, Taxil P (2010) Electrochemical behaviour of thorium(IV) in molten LiF-CaF₂ medium on inert and reactive electrodes. *Electrochim Acta* 55: 4758-4764.
- Hamel C, Chamelot P, Taxil P (2004) Neodymium(III) cathodic processes in molten fluorides. *Electrochim Acta* 49: 4467-4476.
- Chamelot P, Palau P, Massot L, Savall A, Taxil P (2002) Electrodeposition processes of tantalum(V) species in molten fluorides containing oxide ions. *Electrochim Acta* 47: 3423.
- Chamelot P, Lafage B, Taxil P (1997) Using square-wave voltammetry to monitor molten alkaline fluoride baths for electrodeposition of niobium. *Electrochim Acta* 43: 607-616.
- Massot L, Cassayre L, Chamelot P, Taxil P (2007) On the use of electrochemical techniques to monitor free oxide content in molten fluoride media. *J Electroanal Chem* 606: 17-23.